

## Characterization of a *Staphylococcus aureus* Surface Virulence Factor That Promotes Resistance to Oxidative Killing and Infectious Endocarditis<sup>∇†</sup>

Natalia Malachowa,<sup>1,2§</sup> Petra L. Kohler,<sup>3</sup> Patrick M. Schlievert,<sup>3</sup> Olivia N. Chuang,<sup>3</sup> Gary M. Dunny,<sup>3</sup> Scott D. Kobayashi,<sup>1§</sup> Jacek Miedzobrodzki,<sup>2</sup> Gregory A. Bohach,<sup>1‡</sup> and Keun Seok Seo<sup>1\*</sup>

Department of Microbiology, Molecular Biology, and Biochemistry, University of Idaho, Moscow, Idaho 83844<sup>1</sup>; Department of Microbiology, Faculty of Biochemistry, Biophysics and Biotechnology, Jagiellonian University, 30-387 Krakow, Poland<sup>2</sup>; and Department of Microbiology, University of Minnesota Medical School, Minneapolis, Minnesota 55455<sup>3</sup>

Received 8 July 2010/Returned for modification 21 July 2010/Accepted 5 October 2010

***Staphylococcus aureus* is a prominent human pathogen and a leading cause of community- and hospital-acquired bacterial infections worldwide. Herein, we describe the identification and characterization of the *S. aureus* 67.6-kDa hypothetical protein, named for the surface factor promoting resistance to oxidative killing (SOK) in this study. Sequence analysis showed that the SOK gene is conserved in all sequenced *S. aureus* strains and homologous to the myosin cross-reactive antigen of *Streptococcus pyogenes*. Immunoblotting and immunofluorescence analysis showed that SOK was copurified with membrane fractions and was exposed on the surface of *S. aureus* Newman and RN4220. Comparative analysis of wild-type *S. aureus* and an isogenic deletion strain indicated that SOK contributes to both resistance to killing by human neutrophils and to oxidative stress. In addition, the *S. aureus sok* deletion strain showed dramatically reduced aortic valve vegetation and bacterial cell number in a rabbit endocarditis model. These results, plus the suspected role of the streptococcal homologue in certain diseases such as acute rheumatic fever, suggest that SOK plays an important role in cardiovascular and other staphylococcal infections.**

*Staphylococcus aureus* is a commensal that often colonizes skin and mucosal membranes (11, 28). This species is usually benign in healthy individuals, but it is a high-risk pathogen for immunocompromised individuals. As a consequence of its numerous virulence factors and its adaptability, *S. aureus* is one of the most significant human pathogens for both nosocomial and community-associated infections (20). Moreover, an increasing resistance to antibacterial agents and the adaptation and emergence of methicillin- and vancomycin-resistant *S. aureus* (MRSA and VRSA, respectively) strains is alarming (2, 13).

*S. aureus* is the causative agent of diverse human and animal maladies, including, but not limited to, abscesses, food poisoning, toxic shock syndrome, septicemia, and endocarditis (3, 46, 49). This cadre of diseases results from *S. aureus* strain heterogeneity. Although numerous, most *S. aureus* virulence factors are categorized into one of the following groups according to their functions: (i) surface proteins that promote adhesion, internalization, and colonization; (ii) toxins and enzymes that promote tissue damage, inflammation, and invasion and dis-

semination; (iii) surface factors that affect phagocytosis by leukocytes; (iv) factors that enhance survival in phagocytes; or (v) superantigens and other molecules that modulate the immune system by altering the function of lymphocytes and antigen-presenting cells (1, 12, 44).

Our bioinformatics analysis of 13 *S. aureus* genomic sequences in search of potential virulence factors for staphylococcus-induced cardiovascular diseases revealed a conserved open reading frame ([ORF] 96 to 100% identity among all *S. aureus* sequences). The predicted translation products from these ORFs share 59% identity with the 67-kDa myosin cross-reactive antigen (MCRA) of *Streptococcus pyogenes* (19). The *S. aureus* homologue (ORF SA0102) was reported initially by Kuroda et al. (25) in reference to the N315 strain genome sequence. They described SA0102 as one of two major histocompatibility complex class II (MHC-II)  $\beta$ -chain homologues in the N315 genome. The 67-kDa *S. pyogenes* protein and the SA0102 predicted translation product share 62% and 34% similarity (19% and 21.2% identity), respectively, to the murine  $\beta$ 1 domain of the mouse I-A<sup>u</sup> chain (19; also our unpublished results).

The 67-kDa streptococcal homologue is a putative virulence factor, and hybridization studies suggested that related proteins exist in streptococcal groups A, C, and G (19). This protein is a member of extensive MCRA protein family. It reacts with sera from patients with acute rheumatic fever (ARF), acute glomerulonephritis, and active streptococcal infections (19). It also reacts with anti-myosin antibody in sera of patients with ARF. Recently, this streptococcal protein was described as fatty acid double bond hydratase (47). Although members of the MCRA protein family are widely distributed among bacteria, only three proteins from this family have been

\* Corresponding author. Present address: Department of Basic Sciences, College of Veterinary Medicine, Mississippi State University, P.O. Box 6100, Mississippi State, MS 39762. Phone: (662) 325-1419. Fax: (662) 325-1031. E-mail: seo@cvm.msstate.edu.

‡ Present address: Department of Basic Sciences, College of Veterinary Medicine, Mississippi State University, Mississippi State, MS 39762.

§ Present address: National Institute of Allergy and Infectious Diseases, National Institutes of Health, Hamilton, MT 59840.

† Supplemental material for this article may be found at <http://iai.asm.org/>.

<sup>∇</sup> Published ahead of print on 11 October 2010.

TABLE 1. Bacterial strains and plasmids used in this study

Strain or plasmid	Function or relevant properties	Source or reference
<b>Strains</b>		
<i>E. coli</i>		
DH5 $\alpha$	General cloning applications	Life Technologies
BL21(DE3) pLysS	Recombinant protein expression	Stratagene
<i>S. aureus</i>		
Newman	Clinical isolate	ATCC 25904
NM10	Newman <i>sok::Tc</i> ; Tc <sup>r</sup>	This study
NM20	NM10 complemented with the pMIN164- <i>sok</i> plasmid; Tc <sup>r</sup> Em <sup>r</sup>	This study
DU5875	Isogenic mutant of 8325-4; <i>spa::Tc</i> ; Tc <sup>r</sup>	33
RN4220	Restriction negative derivative of 8325-4	24
NM1	RN4220 <i>sok::Tc</i> ; Tc <sup>r</sup>	This study
NM2	NM1 complemented with the pMIN164- <i>sok</i> plasmid; Tc <sup>r</sup> Em <sup>r</sup>	This study
<b>Plasmids</b>		
pDG1515	Source of Tc <sup>r</sup> cassette; Am <sup>r</sup> Tc <sup>r</sup>	14
pSOK1	Plasmid pdg1515 with <i>sok</i> upstream and downstream fragments; Am <sup>r</sup> Tc <sup>r</sup>	This study
pCL10	Temp-sensitive Am <sup>r</sup> Cm <sup>r</sup> Tc <sup>r</sup>	42
pSOK2	Vector pcl10 with <i>sok</i> upstream, downstream, and Tc <sup>r</sup> cassette; Am <sup>r</sup> Cm <sup>r</sup> Tc <sup>r</sup>	This study
pMIN164	<i>E. coli</i> - <i>S. aureus</i> shuttle vector; Am <sup>r</sup> Em <sup>r</sup>	18
pSOK3	Plasmid pMIN164 with <i>sok</i> ORF; Am <sup>r</sup> Em <sup>r</sup>	This study
pGEX-5T	<i>E. coli</i> GST/His-tag vector; Am <sup>r</sup>	5

biochemically characterized (6, 47), and the exact role of the vast majority of proteins and homologues belonging to this family remains unknown. The objective of this study is to characterize the 67-kDa myosin cross-reactive homologue of *S. aureus*. To address this goal, we constructed deletion mutants in two well-characterized *S. aureus* strains, RN4220 and Newman, compared the properties of the parental and mutant strains, and investigated the molecular relatedness of the structural gene in a number of clinical isolates. The data suggest that this protein is ubiquitous among *S. aureus* clinical isolates and could contribute to infectious diseases such as endocarditis by promoting survival in phagocytes and resistance to oxidative killing. Due to the latter property, we tentatively designated the *S. aureus* protein SOK, a surface factor promoting resistance to oxidative killing.

#### MATERIALS AND METHODS

**Bacterial strains, plasmids, and growth conditions.** Strains and plasmids used are described in Table 1. *Escherichia coli* was grown using Luria-Bertani (Difco Laboratories, Detroit, MI) medium that was supplemented with ampicillin (Am; 100  $\mu$ g/ml) or chloramphenicol (Cm; 34  $\mu$ g/ml) when necessary. Except where indicated, *S. aureus* was propagated using tryptic soy (TS) medium (Difco Laboratories, Detroit, MI). Plasmid selection for *S. aureus* was conducted with erythromycin (Em), Cm, or tetracycline (Tc) (5, 10, or 10  $\mu$ g/ml, respectively).

**Bioinformatics analysis.** The search for homologues was performed using BLAST on the NCBI web server (<http://www.ncbi.nlm.nih.gov/>), and sequences were aligned by the ClustalW program (<http://www.ebi.ac.uk/Tools/clustalw/index.html>). The following tools on the ExPASy Proteomic Server were used to analyze various properties of the SOK protein: Compute pI/M<sub>w</sub> was used to calculate isoelectric point and molecular weight, SignalP, version 3.0, was used to calculate the signal peptide cleavage site by artificial neural networks (NN) and hidden Markov models (HMM), ProtScale was used to determine hydrophobicity, and PSIPred was used to determine transmembrane topology (using MEMSAT on the PSIPred Protein Structure Prediction Server). The BPROM program (Softberry, Inc., Mount Kisco, NY) was used to predict bacterial promoter.

**DNA isolation.** Genomic DNA was isolated by using Genomic DNA Prep Plus kits (A&A Biotechnology, Gdynia, Poland) facilitated by a method to promote *S. aureus* lysis (41). Plasmids were isolated with a MiniPrep isolation

kit (Qiagen GmbH, Hilden, Germany) using the manufacturer's protocol. *S. aureus* cells were treated with lysostaphin in the kit resuspension buffer. DNA was quantified using a NanoDrop ND-1000 instrument (Nanodrop Technologies, Wilmington, DE).

**RFLP analysis.** A 1,789-bp fragment containing predicted *sok* coding region plus flanking promoter and ribosome binding sites was amplified using primers 12631 and 12632 (Table 2). PCR products were purified, quantified (see above), and digested with Csp6I, Hin6I, or TaqI. These enzymes were selected based on two criteria: (i) that at least three cleavage sites exist within the PCR-amplified *sok* gene and (ii) that predicted digestion patterns are readily discernible by agarose gel electrophoresis. Fragments were separated by electrophoresis in 2% agarose gels to compare *sok* genotypes according to digestion profiles. At least a one-band difference was used as the criterion for designating unique restriction fragment length polymorphism (RFLP) profiles. Concordance between *spa* typing results and PCR-RFLP was calculated as described previously (30).

**RNA isolation and RT-PCR.** RNA was isolated with an RNeasy Mini Kit (Qiagen Science, Germantown, MD) according to the manufacturer's protocol. Bacteria were disrupted using a FastPrep FP120 homogenizer (ThermoSavant, Holbrook, NY) (45 s at 6.0 m/sec). DNA was removed using RNase-free DNase I (Ambion, Austin, TX), and RNA was further purified by treatment again with the same RNA isolation protocol. RNA samples with a ratio of the optical density at 260 nm (OD<sub>260</sub>)/OD<sub>280</sub> of  $\geq 2.0$  were used. First-strand cDNA was synthesized from 1  $\mu$ g of RNA using Superscript Reverse Transcriptase (Invitrogen, Carlsbad, CA), and 5  $\mu$ l of a 100-fold diluted aliquot was used as the template (final sample volume, 25  $\mu$ l; MicroAmp Optical 96-Well Reaction Plate; Applied Biosystems). Real-time PCR (RT-PCR) was performed in an ABI Prism 7500 system using SYBR green mix as recommended (Applied Biosystems, Foster City, CA).

**Cloning and purification of SOK.** Recombinant SOK (rSOK) was expressed in *Escherichia coli* BL21(DE3) pLysS using pGEX-5T, which expresses proteins with an N-terminal His tag and a glutathione S-transferase (GST) label (5). The predicted SOK ORF was amplified with *Pfu* DNA polymerase (Fermentas, Lithuania); the 1,827-bp product was digested with BamHI and XhoI. The resulting 1,776-bp fragment was cloned into pGEX-5T and transformed into *E. coli* DH5 $\alpha$  cells (Life Technologies, Inc., Gaithersburg, MD). After the appropriate construct was confirmed by PCR and sequencing, the plasmid was purified and transformed into *E. coli* BL21(DE3) pLysS (Stratagene). Expression was induced with 1 mM isopropyl- $\beta$ -D-thiogalactopyranoside (IPTG) when the OD<sub>600</sub> of the culture reached 0.9. Following growth at 20°C for an additional 10 h, cells were collected by centrifugation, washed with phosphate-buffered saline ([PBS] 140 mM NaCl, 2.7 mM KCl, 10 mM Na<sub>2</sub>HPO<sub>4</sub>, 1.8 mM KH<sub>2</sub>PO<sub>4</sub>, pH 7.3), and disrupted using a French press (Thermo Fisher Scientific, Inc.,

TABLE 2. Primers used in this study

Name	Sequence <sup>a</sup>	Purpose <sup>b</sup>
Tet1F	5'-TCAGAATCCAAATCTAGACGAGTGATAAAATTT-3'	Upstream fragment for mutation (XbaI)
Tet1R	5'-ATTTTAATATCTTCGGGATCCACATCGTATTCA-3'	Upstream fragment for mutation (BamHI)
Tet2F	5'-ATTACAATCAATGATTGAATTCGGCAAATGAGTTT-3'	Downstream fragment for mutation (EcoRI)
Tet2R	5'-ATTTCTGTCCCGGTACCATGATTTGAAAT-3'	Downstream fragment for mutation (KpnI)
12631	5'-CTTGGTGGATATGTATTACAGT-3'	PCR-RFLP
12632	5'-TCGTTATAACAATTTGTGTTCTTTT-3'	PCR-RFLP
RT-Fsok	5'-AGCGCCACCAACTGACGA-3'	RT-PCR <i>sok</i> gene
RT-Rsok	5'-CCTGCAAGTGGGTACAGTTTA-3'	RT-PCR <i>sok</i> gene
RT-Fdn	5'-TATTAGGTGTTATTGCAGGTATCGTTG-3'	RT-PCR downstream gene
RT-Rdn	5'-AAATTGGCATTGCATATTCGC-3'	RT-PCR downstream gene
SR4	5'-GGCCTTTGCAGGGCTGGCAAGCCACG-3'	Sequencing of the pGEX-5T insert
SR5	5'-GCTGCATGTGTGTCAGAGGTTTTCACCG-3'	Sequencing of the pGEX-5T insert
MExpF	5'-AAAGGACTTGGGATCCATGATTACAGT-3'	Complementation of <i>sok</i> deletion strains (BamHI)
MExpR	5'-ATAAAAATCTATTAATGGGTCGACTTATAACAAT-3'	Complementation of <i>sok</i> deletion strains (SalI)

<sup>a</sup> Enzyme restriction sites are underlined.

<sup>b</sup> Restriction enzymes used to digest PCR products are in parentheses.

Waltham, MA). rSOK was purified on the glutathione-Sepharose 4B resin, according to the manufacturer's recommendation (Amersham, Piscataway, NJ), and GST label was cleaved with thrombin (Sigma-Aldrich, St. Louis, MO). The recombinant protein was dialyzed against 10 mM morpholinepropanesulfonic acid (MOPS) buffer (pH 7.0) containing 10 mM NaCl and 1 mM EDTA. The apparently pure rSOK, as assessed by SDS-PAGE (26), was stored in dialysis buffer containing 10% glycerol.

**Antibody production.** Sprague-Dawley rats (6 to 8 weeks old; Simonsen Laboratories, Inc., San Diego, CA) were given biweekly subcutaneous injections of rSOK (100 µg) in Freund's incomplete adjuvant (Gibco, Grand Island, NY). One week after the fourth boost, sera were harvested and pooled. The anti-rSOK titer, 15,000, was determined by immunoblotting (9), and diluted (1:10,000) antiserum was typically used for experiments.

**Immunofluorescence analysis of *S. aureus*.** Cell samples were prepared by the method of Hiraga et al. (17). Slides were visualized using a Zeiss LSM 5 Pascal instrument and software (version 4.0, service pack 2; Carl Zeiss MicroImaging GmbH, Heidelberg, Germany) following treatment with anti-rSOK rat serum (see above) and Alexa Fluor 488-conjugated goat anti-rat IgG(H+L) (2 mg/ml) secondary antibodies (Molecular Probes, Inc., Eugene, OR).

**SOK subcellular localization.** Cells and supernatants from overnight (o.n.) cultures (25 ml) were separated by centrifugation (at 8,000 × *g* for 10 min). Culture supernatant proteins were precipitated (2 h at -20°C) with 9 volumes of trichloroacetic acid-acetone (1:8, vol/vol), pelleted, and resuspended in distilled water (1 ml). The cell pellet was washed with deionized water and treated (18,000 lb/in<sup>2</sup>) in a French press (7), followed by the addition of protease inhibitor cocktail and nuclease mix (Amersham Bioscience Corp., Piscataway, NJ) and centrifugation (75,000 × *g* for 30 min). The obtained supernatant containing soluble cytoplasmic proteins was stored at -80°C until needed. The resulting pellet, containing crude membrane and wall fractions, was resuspended in rehydration buffer (7 M urea, 2 M thiourea, 2% amidosulfobetaine-14 [ASB-14], 0.5% Triton X-100, 2 mM tributylphosphine, 1% bromophenol blue), and incubated at room temperature for 2 h. The sample was clarified by centrifugation (75,000 × *g* for 20 min), and supernatant fluids were recovered for analysis of integral membrane proteins. Cell wall proteins in the pellet were released by incubation for 3 h in TE buffer (50 mM Tris-HCl and 10 mM EDTA, pH 8.0) with lysostaphin (40 µg/ml). Proteins were analyzed by SDS-PAGE and immunoblotting (see above).

**SOK deletion mutagenesis.** DNA fragments, 918 (5') and 698 (3') bp in length, were amplified by PCR from within *sok* through external flanking regions. The 5' fragment included nucleotides (nt) -154 through 764; the 3' fragment encompassed nt 1138 through an additional 59 nt after the predicted stop codon (nucleotide numbering is relative to the predicted ATG initiation codon) (see Fig. S1A in the supplemental material). PCR products were digested with appropriate enzymes (Table 2) and ligated on opposite ends of the Tc<sup>r</sup> cassette in pDG1515 (50), resulting in pSOK1 vector. This construct was propagated in *E. coli* DH5α and digested with BamHI and KpnI. The Tc<sup>r</sup> cassette plus flanking *sok* fragments were cloned into the pCL10 shuttle vector, resulting in pSOK2. The plasmid was then electroporated into *S. aureus* RN4220 and Newman as recommended (ECM 600 electroporator; BTX Molecular Delivery Systems). Transformed cells were grown in TS broth (TSB) with Tc (24 h at 43°C) and

plated on TS agar (TSA) containing Tc to select colonies with the first recombination. One colony was transferred to TSB and grown (at 30°C for 5 days) with daily transfer to fresh TSB. After 5 days, an aliquot was grown on TSA with Tc. Colonies were screened for a Tc<sup>r</sup> Cm<sup>s</sup> phenotype indicating that the second recombination resulted in deletion of a 404-nt *sok* sequence and insertion of the Tc cassette. To complement the mutation, a fragment representing the *sok* ORF with 260 nt upstream was amplified using MExpF and MExpR primers and ligated into the BamHI and SalI sites of pMIN164 (18), resulting in pSOK3. This plasmid was electroporated into the *S. aureus* RN4220 and Newman strains (selection was accomplished on TSA with Tc and Em).

**PMN killing assay.** Human polymorphonuclear leukocytes (PMNs) were isolated from heparinized venous blood of four different donors in accordance with a human subject protocol approved by the University of Idaho Institutional Review Board for Human Subjects (approval number 05-056). Donors were informed of the procedure risks and provided a written consent prior to participation. Killing of bacteria by human PMNs was determined as described previously (22), with the following modifications. PMNs (10<sup>6</sup>) were combined with opsonized bacteria (10<sup>7</sup>) in 96-well plates which were centrifuged at 400 × *g* for 5 min, followed by incubation at 37°C for 15 min. PMNs were treated with 400 µM gentamicin (Sigma-Aldrich Co.) for 10 min to remove any remaining extracellular bacteria (time [T] zero). Cultures were further maintained for time points up to 180 min. At the times indicated in Fig. 3A, gentamicin was removed by aspiration, and cells were gently washed with PBS and lysed in sterile water, and the bacteria were plated on TSA. CFU were enumerated following overnight incubation, and the percentage of bacteria killed was calculated using the following equation: (CFU<sub>PMN+</sub>/CFU<sub>T=0</sub>) × 100, where CFU<sub>T=0</sub> indicates number of enumerated colonies for time point zero and CFU<sub>PMN+</sub> is the number of CFU for each analyzed time point. The assay measures the percentage of the total number of viable ingested bacteria compared to the number at time point zero.

**ROS analysis.** Human PMNs (see above) were mixed with 10 mM 2,7-dichlorodihydrofluorescein diacetate (DCF) (Molecular Probes Inc., Eugene, OR) and incubated for 30 min at room temperature in the dark (8). Opsonized bacteria (above) were mixed with the PMNs at a 10:1 ratio, and transferred to precoated wells of a 96-well plate. The plate was centrifuged (for 5 min at 700 × *g* at 4°C) to synchronize phagocytosis. Reactive oxygen species (ROS) production was monitored during incubation (at 37°C) using a SpectraMax M2 plate reader (Molecular Devices, Sunnyvale, CA) with 485-nm excitation and 538-nm emission wavelengths. Data were analyzed by SoftMax Pro software, version 5.0.1 (Molecular Devices), and are presented as the rate of change (*V*<sub>max</sub>) in fluorescence over time.

**H<sub>2</sub>O<sub>2</sub> and <sup>1</sup>O<sub>2</sub> susceptibility assays.** *S. aureus* cells (mid-exponential growth phase) were harvested by centrifugation, washed once with PBS, and adjusted to 1 × 10<sup>8</sup> and 2 × 10<sup>9</sup> cells/ml, respectively, for H<sub>2</sub>O<sub>2</sub> and <sup>1</sup>O<sub>2</sub> assays (27). To assess the effect of H<sub>2</sub>O<sub>2</sub> on *S. aureus* viability, the bacteria were incubated with various concentrations of H<sub>2</sub>O<sub>2</sub> (Sigma-Aldrich Co., St. Louis, MO) in glass tubes for 1 h at 37°C, followed by addition of *Micrococcus lysodeikticus* catalase (1,000 U/ml) (Sigma-Aldrich Co.) to quench the remaining H<sub>2</sub>O<sub>2</sub>. The percentage of surviving bacteria was calculated by using the following equation: (CFU<sub>H<sub>2</sub>O<sub>2</sub>+</sub>/CFU<sub>T=0</sub>) × 100, where CFU<sub>T=0</sub> indicates number of enumerated

TABLE 3. Comparison of *sok* PCR-RFLP results with *spa* typing<sup>a</sup>

<i>spa</i> cluster	<i>sok</i> PCR-RFLP pattern				Isolate no. or name (country/yr) <sup>b</sup>
	Type	Csp6I	Hin6I	TaqI	
S1	1	A	A	A	2233 (PL/97), 2234b (PL/98), 2255 (PL/98), 2258 (PL/98), 2577 (PL/98), 303 (PL/00), 2260 (PL/98), 3028 (PL/96), 3498 (RU/98), 3521 (LT/98), NCTC8325 <sup>c</sup>
S2	2	B	B	B	N104A (PL/95), 1791 (PL/97), 1794 (PL/97), 1807 (PL/97), 3254 (TR/96), MR1003 (PL/92), 2689 (PL/98), N98 (PL/95), MR11 (PL/92), MR1064 (PL/92), MR89 (PL/92), B098 (PL/94), A005b (PL/94), 3497 (BG/98), MR47 (PL/92), MR76 (PL/92), J405 (PL/94), 771 (PL/97), 3301 (SL/98), 2690 (PL/98), 3121 (PL/96), H390 (PL/94), 3248 (CZ/96), EMRSA-16 (UK/92), 2956 (PL/01), 2684 (PL/98) <sup>c</sup>
S2	3	B	D	B	C115 (PL/94), 2688 (PL/98), A005a (PL/98)
S3	4	C	C	E	1899 (PL/96), 2838 (PL/96), MR1010A (PL/92)
	5	B	C	E	3502 (BG/98)
	6	B	B	C	794 (PL/97) <sup>c</sup>
S4	7	C	C	D	3483 (SL/98), MR44 (PL/92), MR63 (PL/92), MR84 (PL/92), MR5 (PL/92), MR24 (PL/92), MR52 (PL/92), 2700 (PL/98), MR31 (PL/92), MR29 (PL/92), MR27 (PL/92), MR80 (PL/92), N39 (PL/95)
t159 <sup>d</sup>	8	B	C	B	BN4 (PL/96)

<sup>a</sup> *spa* typing results used in this table were previously published by Malachowa et al. (30).

<sup>b</sup> Countries are abbreviated as follows: BG, Bulgaria; CZ, Czech Republic; LT, Lithuania; PL, Poland; RU, Russia; SL, Slovenia; TR, Turkey; UK, United Kingdom. Years are abbreviated by the last two digits (e.g., 97 is 1997 and 00 is 2000).

<sup>c</sup> Methicillin-susceptible *S. aureus* strain.

<sup>d</sup> The BN4 strain does not belong to any *spa* cluster; the *spa* type is t159.

colonies for time point zero and CFU<sub>H<sub>2</sub>O<sub>2</sub>+</sub> is number of CFU after incubation with H<sub>2</sub>O<sub>2</sub> for 1 h. For <sup>1</sup>O<sub>2</sub> susceptibility, bacteria were incubated in 24-well plates (for 30 or 60 min at 37°C) with various concentrations (0.25 to 6.0 µg/ml) of methylene blue (Sigma-Aldrich Co.). The plates were placed 10 cm from a 100-W incandescent light bulb, and survival was measured by plate counting.

**Endocarditis model.** New Zealand White rabbits (2 to 3 kg) were anesthetized with xylazine and ketamine (20 mg/kg each) and subjected to transaortic catheterization for 2 h to damage the aortic valves (43). After the catheters were removed and animals were closed, a washed suspension of *S. aureus* (2 ml; 1.0 × 10<sup>9</sup>/ml for RN4220 strains or 5.0 × 10<sup>8</sup>/ml for Newman strains in PBS) was administered to each rabbit in the marginal ear vein. Animals were observed daily. Except for rabbits infected with the parental Newman strain, which succumbed on days 2 and 3, animals were sacrificed on days 4 and 5 to assess vegetation formation. Aseptically harvested vegetations from all animals were weighed, and bacteria were enumerated by plate counts.

**Statistical analysis.** A Student *t* test was carried out using GraphPad Prism software, version 4.02 (GraphPad Software, Inc., San Diego, CA).

## RESULTS

**Bioinformatics analysis results.** The initial analysis of published *S. aureus* genome sequences revealed that the *sok* gene is ubiquitous and that the sequence is highly conserved in these strains (96 to 100%). In all 13 strains, a 591-residue protein is predicted to be translated from a 1,776-bp gene (see Fig. S1A in the supplemental material). The theoretical isoelectric point (pI) and molecular mass of the *S. aureus* Newman *sok* translation product are 5.0 and 67,648 Da, respectively. A potential signal peptide cleavage site predicted using the neural networks (NN) algorithm is located between positions 36 and 37 (SLA-AA). Subsequent to the removal of the potential signal peptide, the deduced molecular size of the putative mature SOK protein in the Newman strain is 63,663 Da. One potential transmembrane-spanning region contains an internal helix cap (residues 25 to 28), a central transmembrane helix (residues 29 to 38), and an external helix cap (residues 39 to 42). This is consistent with the hydrophobicity profile of SOK, which predicts a highly hydrophobic region between residues 25 and 42 (results not shown). In the *S. aureus* Newman sequence (accession number AP009351) (4), *sok* is located between ORFs

for two hypothetical proteins (NWMN0049 and NWMN0051), which by BLAST sequence comparison resemble a Na/P co-transporter and metabolic/drug transporter, respectively. *sok* homologues are found in a variety of genome sequences including those of Gram-positive and Gram-negative bacteria (see Fig. S1B in the supplemental material, created using MEGA software [45]). *S. aureus* SOK sequences share 89.9 to 91.2% homology with homologues in other staphylococcal species and >33.8% homology with those of other bacterial species (see Fig. S1B).

**RFLP analysis.** The molecular genetic variability of *sok* was evaluated using an RFLP technique to analyze a 59-member culture collection (National Institute of Public Health, Warsaw, Poland) comprised predominantly of methicillin-resistant and methicillin-sensitive *S. aureus* human clinical isolates. The isolates are from a variety of human infections, predominantly from Poland but also from other European countries collected from 1992 through 2001. Initial characterization of these isolates by pulsed-field gel electrophoresis (PFGE), PCR typing, multilocus sequence typing (MLST), and *spa* typing was previously reported (30). RFLP analysis of the *sok* locus reveals that the 59 isolates segregate into eight unique RFLP types, and this segregation correlates closely with the clustering of *spa* types (Table 3). RFLP analysis of the *sok* gene reveals 97% concordance with *spa* clusters deduced previously by Malachowa et al. (30). The largest RFLP group correlates with the S2 *spa* cluster that includes 44% of all isolates. This particular *spa* cluster contains *spa* types comprised of the identical or similar repeat profiles (23, 30). Nearly all *sok* RFLP patterns correlate with a specific *spa* cluster with two exceptions: isolates 794 and 3502 belong to the S3 cluster, yet they fell into different groups by RFLP analysis of the *sok* locus. Only the BN4 isolate was not classified to any cluster type, either by *spa* typing or *sok* PCR-RFLP.

**SOK is surface exposed and copurifies with membrane fractions.** The *sok* gene in *S. aureus* strain Newman was disrupted

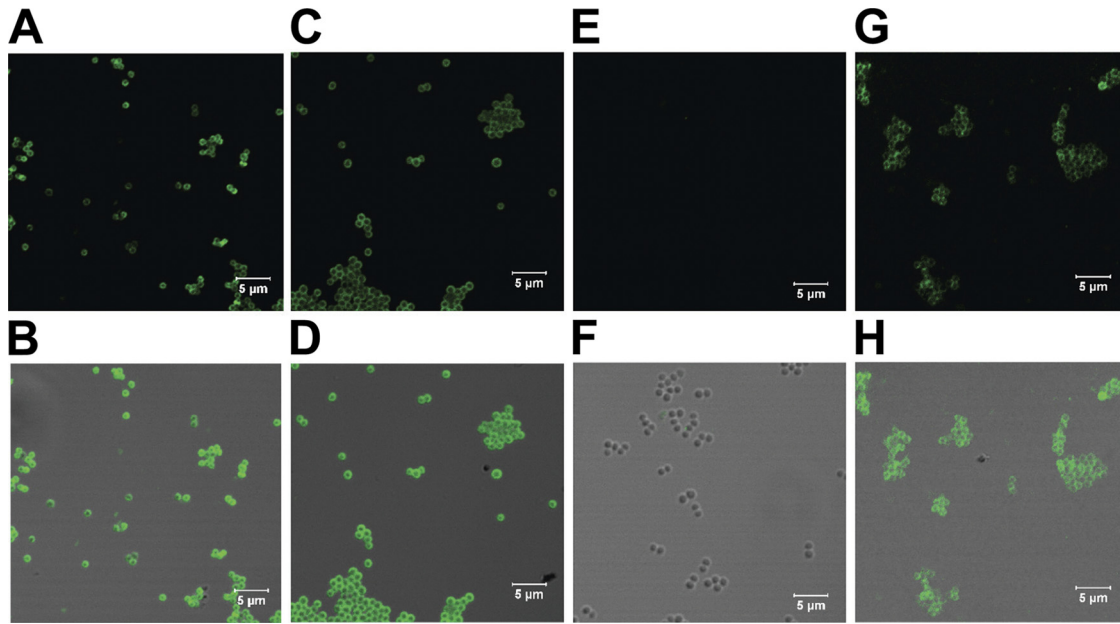


FIG. 1. Surface localization of SOK. *S. aureus* bacterial strains DU5875 (A and B), Newman (C and D), NM10 (E and F), and NM20 (G and H) (magnification of  $\times 227$ ) were observed by immunofluorescence using SOK-specific rat antiserum, followed by Alexa Fluor 488-conjugated goat anti-rat Ig(H+L) secondary antibody (A, C, E, and G) or combined fluorescence with differential interference contrast (B, D, F, and H).

with a  $Tc^r$  cassette introduced by allelic replacement, as described previously, to generate strain NM10 ( $\Delta sok$ ). Strain NM10 was transformed with a plasmid harboring the promoter region plus the coding region of *sok* to produce the complemented strain designated NM20. RT-PCR confirmed the lack and restoration of detectable *sok* expression in the mutant and complemented strains, respectively, plus the absence of any detectable effect on expression of the adjacent downstream gene (results not shown).

Gene expression studies were consistent with immunofluorescence microscopy using rat antiserum prepared against rSOK. The Newman, NM10, and NM20 strains and a strain lacking protein A (DU5875) were examined for SOK by immunofluorescence microscopy (Fig. 1). The *S. aureus* parental and complemented strains expressed detectable levels of SOK on the cell surface. SOK was also detectable on the surface of the strain lacking protein A. In contrast, SOK was not detected on the surface of the *sok* deletion strain (Fig. 1).

Proteins in culture supernatants and subcellular fractions were resolved by SDS-PAGE (Fig. 2A) and analyzed by immunoblotting (Fig. 2B). The SOK protein was detected in integral membrane fractions but not in fractions containing cytoplasmic proteins or proteins covalently bound to the cell wall (Fig. 2). The membrane fraction contained an immunoreactive band with a migration consistent with a  $\sim 55$ -kDa protein, which is smaller than predicted (67.6 kDa) based on bioinformatic analysis (see above). Internal controls for an extracellular protein (ScpA, 44 kDa), an integral membrane protein (AgrC, 42 kDa), and a covalently bound membrane protein (SrtA, 24 kDa) were appropriately detected from the corresponding protein fractions (Fig. 2C).

**SOK affects *S. aureus* survival and ROS production in PMNs.** Human PMNs were cultured under conditions to promote synchronized phagocytosis of opsonized *S. aureus*. After

15 min, extracellular bacteria were killed with gentamicin, and the percentages of viable intracellular bacteria were quantified after incubation for additional time periods. The parental strain displayed nearly linear killing kinetics throughout the 3-h incubation period following addition of gentamicin, after

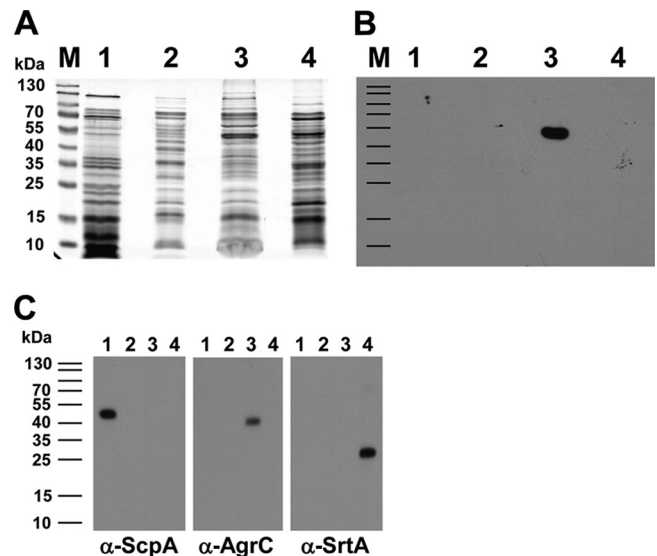


FIG. 2. Subcellular localization of SOK in *S. aureus* Newman using SDS-PAGE (A), immunoblotting with anti-rSOK rat antiserum (B), and immunoblotting with control antibodies (for extracellular protein, anti-ScpA; for integral membrane protein, anti-AgrC; and for covalently bound protein, anti-SrtA) (C). Subcellular localization of SOK was assessed using various bacterial cellular proteins. Lanes M, Page-Ruler Prestained Protein Ladder (Fermentas); lanes 1, extracellular proteins; lanes 2, cytoplasmic fraction; lanes 3, integral membrane fraction; lanes 4, covalently bound proteins.  $\alpha$ , anti.

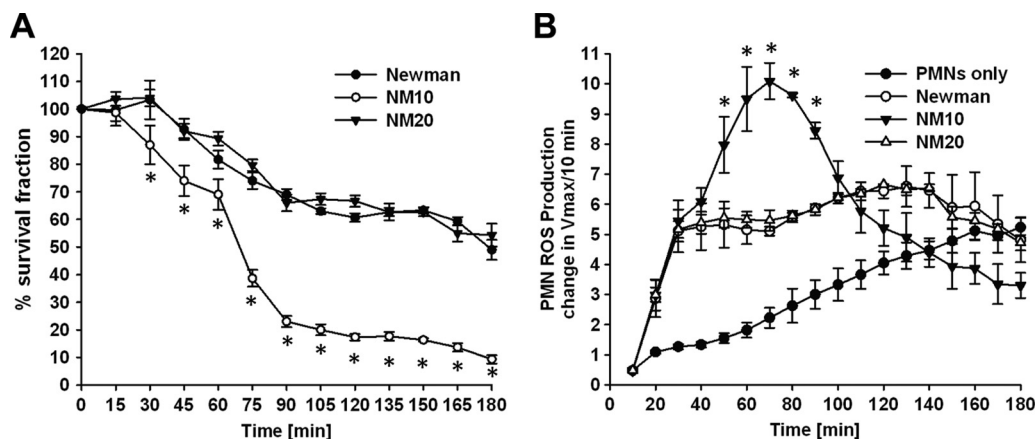


FIG. 3. *sok* affects interactions of *S. aureus* with PMNs. To assess the effect of *sok* on innate immunity, we measured bacterial survival in PMNs and ROS production in PMNs. (A) For the survival assay, PMNs were incubated with opsonized *S. aureus* for 15 min to allow engulfment of bacteria and for an additional 10 min at 37°C with gentamicin prior to commencement of the assay ( $T = 0$ ). The PMNs were then incubated for up to 180 min. Data shown are the means of four experiments which were performed in triplicate ( $n = 12$ ). Statistical significance ( $P < 0.01$ ) between the Newman and NM10 strains is indicated by asterisks. (B) The ROS production is shown as a second-order kinetics plot of the maximum increase in fluorescence ( $V_{max}$ ) over 10-min intervals up to 180 min. Data shown are the means of four experiments which were performed in triplicate ( $n = 12$ ). For each experiment PMNs and sera were isolated from four different donors. Statistical significance ( $P < 0.01$ ) between Newman and NM10 is indicated by asterisks.

which 43.7% of intracellular bacteria remained viable (Fig. 3A). The isogenic *sok* deletion strain (NM10) was more sensitive to PMN killing: 49.5% of bacteria were killed after 65 min, and after 3 h, only 12.7% remained viable. The complemented strain (NM20) showed killing kinetics similar to that of the parental strain.

Disruption of the *sok* gene affected the PMN ROS production following phagocytosis of *S. aureus* Newman. Phagocytosis of the parental Newman isolate rapidly induced PMN ROS production compared to resting PMNs (Fig. 3B). Interestingly, ROS levels in cultures harboring phagocytosed *S. aureus* bacteria lacking SOK were dramatically different from levels in cultures containing the parental strain (Fig. 3B). Despite nearly identical levels of ROS for the first 40 min, levels rose dramatically for the next 30 min until they eventually declined to levels at or below those of PMN cultures harboring the phagocytosed Newman parental strain. The pattern of ROS production was restored to the parental strain by SOK complementation.

**SOK affects *S. aureus* sensitivity to  $^1\text{O}_2$  killing but not  $\text{H}_2\text{O}_2$ .** Since SOK expression influenced ROS levels and survival in PMNs harboring intracellular staphylococci, we assessed whether SOK expression affects susceptibility to the ROS molecules  $\text{H}_2\text{O}_2$  or  $^1\text{O}_2$ . Analysis of the bacterial cell viability of the Newman and NM10 strains after 1 h of incubation with various concentrations of  $\text{H}_2\text{O}_2$  indicated that SOK expression did not affect the viability of *S. aureus* cells when they were exposed to  $\text{H}_2\text{O}_2$ . All strains showed dose-dependent killing effects with respect to increasing concentrations of  $\text{H}_2\text{O}_2$ . Following exposure to 10 mM  $\text{H}_2\text{O}_2$ , all strains showed approximately 50% survival ( $49.5\% \pm 10.3\%$ ,  $53.8\% \pm 4.3\%$ , and  $53.1\% \pm 6.1\%$  for Newman, NM10, and NM20, respectively). Following exposure to 100 mM  $\text{H}_2\text{O}_2$ , all strains showed approximately 5 to 6% survival ( $5.6\% \pm 0.68\%$ ,  $6.6\% \pm 1.2\%$ , and  $5.5\% \pm 0.95\%$  for Newman, NM10, and NM20, respectively) (Fig. 4A).

Although *sok* did not affect survival of bacteria during incubation with  $\text{H}_2\text{O}_2$ , additional experiments indicated that the *sok* deletion strain was more sensitive to  $^1\text{O}_2$  than the parental strain (Fig. 4B and C). Methylene blue releases singlet oxygen ( $^1\text{O}_2$ ) species when exposed to light and was therefore used to measure the susceptibility of *S. aureus* strains to  $^1\text{O}_2$ . In the presence of 0.5 and 1  $\mu\text{g}/\text{ml}$  methylene blue for a 60-min incubation time, the survival rates of both strains dropped significantly, compared to the same concentration of methylene blue for a 30-min incubation. The strain lacking SOK (NM10) was 4 and 24 times more sensitive to  $^1\text{O}_2$  than the parental strain after incubation for 30 min with 0.5 and 1  $\mu\text{g}$  of methylene blue, respectively. The highest level (498 times) of difference in susceptibilities to  $^1\text{O}_2$  between mutant and wild-type strains was observed when bacteria were incubated with 1  $\mu\text{g}$  of methylene blue for 60 min. Longer incubation times (2 and 3 h) as well as higher concentrations of methylene blue (3 and 6  $\mu\text{g}/\text{ml}$ ) were tested for the Newman and NM10 strains, but no bacteria were able to survive under such conditions (results not shown).

**SOK enhances virulence in a model of staphylococcal endocarditis.** To investigate the effect of *sok*, and thus SOK, on virulence of *S. aureus*, an infective endocarditis model was used. New Zealand White rabbits with aortic valve leaflets previously damaged by cardiac catheterization were challenged with the parental *S. aureus* strain RN4220 or Newman or with *sok* deletion derivatives of the parent strains (NM1 or NM10, respectively). Animals were also challenged with *sok* deletion strains complemented with a plasmid encoding *sok* (NM2 or NM20). Rabbits were challenged intravenously with  $1 \times 10^9$  CFU of Newman or Newman derivatives. RN4220 and its derivatives were used to infect rabbits at a dose of  $2 \times 10^9$  CFU per animal. Hearts were harvested immediately from animals that died and from survivors that were euthanized after infection. Heart tissues were examined, and vegetations on aortic valves were removed, weighed, and homogenized to

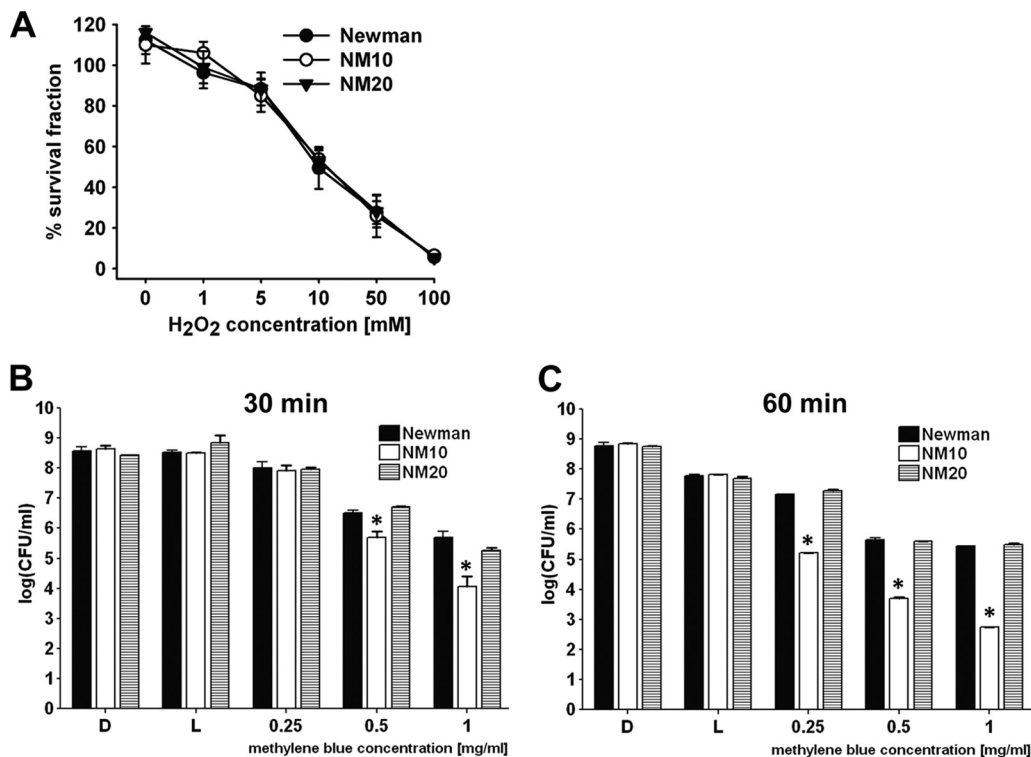


FIG. 4. *sok* affects susceptibility to <sup>1</sup>O<sub>2</sub> but not H<sub>2</sub>O<sub>2</sub>. (A) The susceptibility of various strains (Newman, NM10, and NM20) to treatment with various concentrations of H<sub>2</sub>O<sub>2</sub> was measured by enumeration of CFU after incubation with H<sub>2</sub>O<sub>2</sub>. (B and C) The susceptibility of various strains (Newman, NM10, and NM20) to methylene blue-producing <sup>1</sup>O<sub>2</sub> by photoactivation was measured by enumeration of CFU after 30 min or 60 min. Two controls (L, incubation under a direct light source without methylene blue; D, incubation in darkness without methylene blue) were included for each experiment. Data shown are the means of four experiments which were performed in triplicate ( $n = 12$ ). Statistical significance ( $P < 0.01$ ) between the Newman and NM10 strains is indicated by asterisks.

enumerate the bacteria contained in the vegetations. If vegetations were not observed, the aortic valves were removed from hearts and homogenized to enumerate bacteria adhering to host tissue.

Infection with parent *S. aureus* RN4220 caused vegetations in all animals ( $45.2 \pm 5.1$  mg). In contrast, vegetations were observed in only one of six rabbits infected with NM1 (a *sok* deletion strain) (6.0 mg) (Fig. 5A). Animals infected with the parental RN4220 strain showed greater weight loss than animals infected with NM1 and had diarrhea and mottled faces (Fig. 5B). Vegetations were also observed in animals infected with the complemented strain (NM2) ( $40.0 \pm 7.9$  mg). Statistical analysis of the vegetation sizes by an unpaired *t* test showed that the parental RN4220 strain and NM2 strain produced vegetation sizes that were significantly larger ( $P < 0.0001$  and  $P = 0.0003$ , respectively) than the vegetations produced by the *sok* deletion mutant but not significantly different ( $P = 0.58$ ) from each other. Consistent with vegetation sizes, *S. aureus* RN4220 and NM2 also produced vegetations with larger bacterial loads ( $\log_{10}$  CFU of  $4.90 \pm 0.35$  and  $3.71 \pm 0.71$ /heart, respectively) than the *sok* mutant ( $\log_{10}$  CFU of  $1.49 \pm 0.18$ /heart). As measured by an unpaired *t* test, the bacterial loads of vegetations produced by RN4220 and NM2 were significantly different from the bacterial loads of vegetations produced by the *sok* deletion mutant NM1 ( $P < 0.00001$  and  $P < 0.007$ , respectively).

Infection with parent strain Newman and the *sok* deletion

mutant NM10 produced vegetations in all infected animals, but vegetations produced by the Newman strain were significantly larger than vegetations produced by NM10 as measured by a *t* test ( $87.0 \pm 24.0$  mg and  $7.0 \pm 6.6$  mg, respectively;  $P < 0.01$ ). Statistical analysis by an unpaired *t* test showed that the bacterial load of vegetations produced by the Newman strain ( $\log_{10}$  CFU of  $7.31 \pm 0.74$ /heart) was significantly higher than the bacterial load of vegetations produced by strain NM10 ( $\log_{10}$  CFU of  $4.02 \pm 1.24$ /heart;  $P < 0.05$ ). Infection with the complemented strain, NM20, caused vegetations with bacterial loads statistically similar to those of the parental Newman strain ( $\log_{10}$  CFU of  $6.71 \pm 0.80$ /heart;  $P < 0.6$ ).

## DISCUSSION

This study characterized the molecular and biological properties of an *S. aureus* protein tentatively designated SOK. The protein was designated SOK to highlight its cell surface location and enhancement of resistance to oxidative killing. *In silico* sequence analysis for potential staphylococcal virulence factors involved in systemic or cardiovascular infections identified SOK, partly because of its relatedness to the *S. pyogenes* 67.7-kDa myosin cross-reactive protein. SOK has not been extensively studied but was previously noted during the report of the *S. aureus* N315 genome sequence (25). The N315 SOK is encoded by ORF SA0102 and was described as an MHC-II  $\beta$ -chain homologue. SOK and its *S. aureus* homologues share

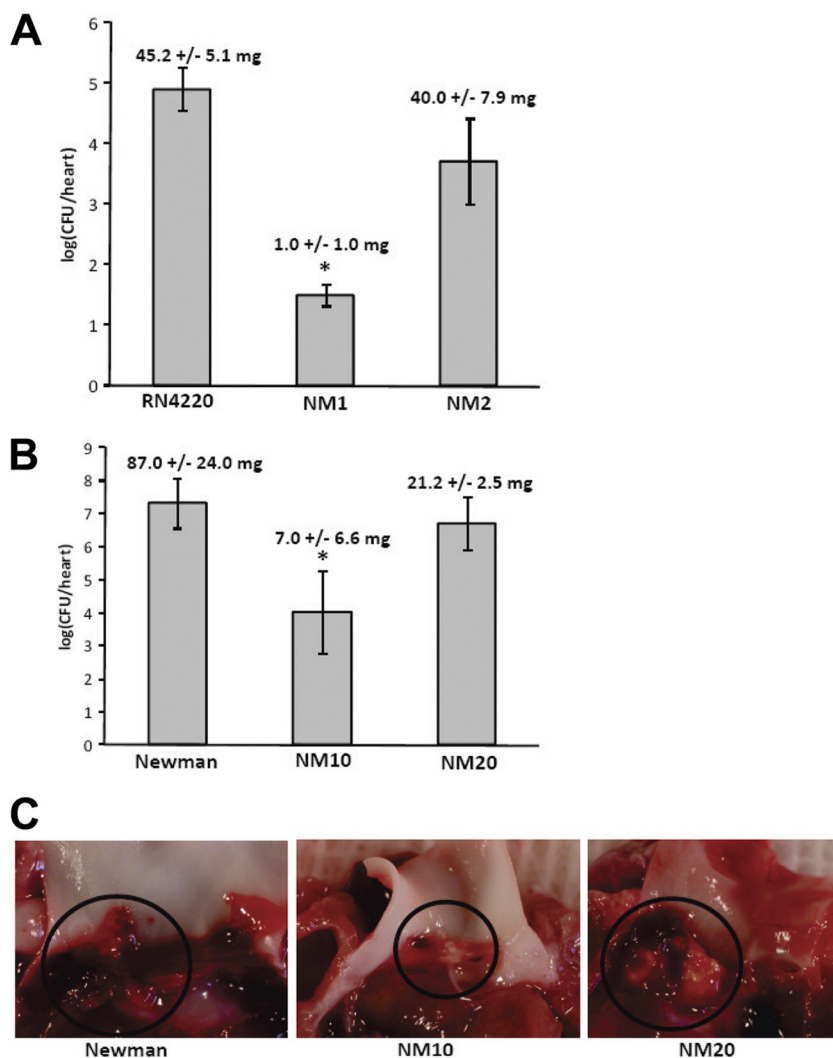


FIG. 5. SOK expression contributes to endocarditis vegetation formation. The rabbit model of endocarditis was used to examine the ability of RN4220 and RN4220-derived strains (NM1 and NM2) (A) or Newman and Newman-derived strains (NM10 and NM20) (B) to form vegetations on heart valves. Bacteria in vegetations or adhering to heart valves were enumerated, and vegetations were weighed. The mean weight of vegetations produced by each strain is indicated at the top of the bar for each strain. Statistical significance ( $P < 0.05$ ) between the wild type and mutant is indicated by asterisks. (C) Representative vegetations from infections with strains Newman, NM10, and NM20 were photographed. Vegetations adhering to heart valves are indicated with circles. Vegetations from animals infected with Newman or NM20 were larger than vegetations from animals infected with NM10.

20 to 21% identity and 34% similarity to murine HLA class II  $\beta$ -chain homologues (RefSeq NP\_996988) on the almost 300-residue-long fragment (unpublished data).

SOK has homologues in other bacteria and shares 49.8 to 62.3% sequence homology with proteins in *Bacillus*, *Bradyrhizobium*, *Bifidobacterium*, *Clostridium*, *Enterococcus*, *Lactococcus*, *Lactobacillus*, *Leuconostoc*, *Streptococcus*, and *Rhodopseudomonas* genera and less, but significant, relatedness to numerous homologues in other Gram-positive and Gram-negative bacteria species (see Fig. S1B in the supplemental material). SOK and its relatives have several conserved sequences which, in SOK, encompass residues 75 to 102, 174 to 211, and 495 to 539, showing >90% homologies. Previously, the most well-characterized protein in this family was the *S. pyogenes* 67-kDa myosin cross-reactive antigen (19, 47), which reacts with sera from patients with streptococcal infections and post-

streptococcal sequelae (19). Considering the numerous SOK homologues and various degrees of relatedness, plus the unique association of *S. pyogenes* with immunopathologies, the ability to cross-react with myosin antibodies may be unique to the streptococcal homologue. Studies to determine whether other SOK homologues possess this property are ongoing in our laboratories.

This high level of sequence conservation is also reflected in PCR-RFLP results, which generated only eight different pattern types among a collection of 59 clinical isolates digested with three different restriction endonucleases. The PCR-RFLP results for *sok* were compared with *spa* typing results, which were previously reported for these same isolates (30). The *spa* typing method was chosen here as one of the most suitable techniques for evaluation of long-term evolutionary changes (15, 40). The differences between RFLP patterns reflect the



variability of the *sok* gene among the 13 sequenced *S. aureus* genomes analyzed, where this variability is caused by point mutations in *sok* (data not shown). Nearly 97% concordance between deduced *spa* typing clusters and *sok* PCR-RFLP groups illustrates the significance of the *sok* gene for staphylococcal epidemiology. It is possible that the high concordance between *spa* typing and *sok* PCR-RFLP is the result of the close genetic linkage of these two genes. In the majority of sequenced *S. aureus* genomes, these two genes are separated by less than 7.5 kb, including four ORFs, and in some genomes, such as those of the MW2 and MSSA476 strain, these two genes are separated by less than 3 kb, which include only two ORFs (4, 25).

Consistent with immunoblotting results showing colocalization of SOK in the membrane fractions, immunofluorescence experiments indicated that SOK is exposed on the *S. aureus* cell surface. However, sequence analysis did not reveal the presence of a typical LPXTG cell wall-anchoring motif although SOK has one predicted N-terminal transmembrane domain encompassing residues 25 through 42 within a potential signal peptide sequence (10). Repeated attempts to obtain a pure or partially purified mature form of SOK for the purpose of N-terminal sequencing to help explain the size discrepancy between bioinformatic analysis (~67.6 kDa) and immunoblotting results (~55 kDa) were unsuccessful. Thus, whether SOK has a signal peptide which is removed during maturation and localization is still to be resolved. It has been shown that staphylococcal proteases such as metalloprotease and metallo-cysteine protease are involved in the maturation process for staphylococcal virulence factors such as lipase and serine protease (35, 38). It is possible that SOK might be processed by staphylococcal protease in the maturation and localization process. This possibility is currently under investigation.

One striking effect of SOK is its ability to confer resistance to killing by PMNs following phagocytosis. The mechanism by which SOK could contribute to virulence is not completely understood but likely is due at least partly to its role in promoting survival in phagocytes, mediated by the resistance to PMN oxidative killing. The human innate immune response is an essential first line of defense against bacterial pathogens (16, 21, 39, 44). PMNs are recruited early to sites of infection and typically efficiently recognize and ingest invading *S. aureus*. The ability of PMNs to kill *S. aureus* is based on the bactericidal activity of ROS produced by the NADPH-dependent oxidase and antimicrobial compounds contained within granules. The importance of ROS in protection against *S. aureus* is exemplified by the increased susceptibility of NADPH oxidase-deficient chronic granulomatous disease patients to severe staphylococcal infections. To test the involvement of SOK in resistance to the innate immune response, PMN bactericidal activity was assessed following phagocytosis of a serum-opsonized *S. aureus* Newman wild-type strain and an isogenic *sok* mutant derivative. Our data indicate that survival of the *S. aureus sok* mutant strain in human PMNs was decreased compared to survival of the isogenic parent strain at all times tested. In addition, PMN ROS production was increased following interactions with the *S. aureus sok* deletion strain compared to that induced by the wild-type strain. Further examination of the role of SOK in ROS resistance indicates that SOK is involved in resistance to singlet oxygen and not hydro-

gen peroxide. Inasmuch as our study demonstrates that SOK is localized to the cell surface of *S. aureus* and that the mutant strain elicits altered PMN ROS production, it is possible that SOK participates in pathogen recognition by neutrophils. However, efficient PMN ROS production and killing in response to wild-type strains of *S. aureus* have been demonstrated previously (36, 48). It is also possible that the apparent increase in the PMN oxidative burst following interactions with the *sok* mutant strain is due to alterations in metabolic pathways controlling the *S. aureus* oxidative stress response. *S. aureus* has been shown to produce both catalase and superoxide dismutase in response to oxidative stress (29). Increased production of either enzyme following ingestion by PMNs would result in a decrease in oxidation of the DCF substrate in the *in vitro* ROS assay. Alternatively, the differential effects in ROS levels in cells following the parental versus deletion mutant could be the result of more efficient quenching of singlet oxygen by the parental strain. There are a number of additional reactive oxygen species that are present in the phagosome of polymorphonuclear phagocytes. Activation of the NADPH oxidase generates superoxide, a relatively unstable molecule that rapidly dismutates itself to form hydrogen peroxide and oxygen (or is catalyzed by superoxide dismutase). The diversity of ROS present in the phagosome, in addition to relative instability, confounds simulation of this environment through use of independent compounds. In addition, the direct role of ROS in microbicidal activity has been intensely debated (34). At the very least, PMN microbicidal activity is likely the result of integrated activities of both oxygen-dependent and -independent molecules. In our study we tested directly the ability of the *S. aureus*  $\Delta sok$  strain to survive following neutrophil phagocytosis through *in vitro* killing assays. It is unclear whether the ability of the *S. aureus*  $\Delta sok$  strain to alter PMN ROS production kinetics and the increased sensitivity to singlet oxygen/PMN killing are linked.

With use of deletion mutagenesis, we demonstrated that SOK affects *in vivo* staphylococcal virulence. Under the conditions tested, the lack of the SOK protein severely debilitated the virulence of two *S. aureus* strains tested in the rabbit endocarditis model. Vegetation formation was completely abrogated or reduced to minimal levels, and the number of culturable bacteria in the hearts was reduced by several logs. We hypothesize that the inability of the SOK-deficient strains to cause vegetations as significant as those formed by the parent and complemented strains is due to their increased elimination before vegetations can form. This is consistent with our prior studies with *Enterococcus faecalis*, related to the surface protein enterococcal aggregation substance, where it has been shown that the aggregation substance also interferes with phagocyte killing (37) and contributes significantly to vegetation formation (43). Our prior studies also suggest that once vegetations begin to form in *E. faecalis* endocarditis, the enterococci become trapped within host- and bacterium-derived matrices that significantly reduce phagocytic removal (32). Interestingly, McAleese et al. (31) demonstrated that *sok* expression was elevated 2.6-fold in isolates from a heart valve compared to bloodstream isolates of the same patient. The reduced ability of *sok* deletion strains to form vegetations suggests that *sok* expression may be important as *S. aureus* interacts with host cells in heart tissues.

Collectively, this study resulted in partial biochemical and biological characterization of the SOK protein. Certainly, to get a full characterization of the SOK protein and its complete role in *S. aureus* infections further investigation is required. SOK protects bacteria during the infection process from neutrophil killing, as well as promoting vegetation formation during heart infections. The presence of *sok* homologues in a diverse group of organisms that includes both pathogens and environmental bacteria suggests that SOK and its homologues may function to protect bacteria from ROS encountered both in animal hosts and in the environment.

#### ACKNOWLEDGMENTS

These studies were supported by the Idaho Agricultural Experiment Station in addition to the following: Committee for Scientific Research grant PBZ-KBN-101/T09/2003/14 (J.M.) and Public Health Service grants P20-RR016454 (G.A.B.), P20-RR15587 (G.A.B.), and AI074283 (P.M.S.); U.S. Department of Agriculture NIFA AFRI grant 2008-35204-04582 (K.S.S. and G.A.B.); and National Centers for Research Resources, Centers of Biomedical Research Excellence, grant P20RR015587 (S.K.). P.M.S. also acknowledges membership in and support (U54 AI57153) from the Region V Great Lakes Regional Center of Excellence in Biodefense and Emerging Infectious Diseases Consortium.

We are grateful to Waleria Hryniewicz (National Medicines Institute, Warsaw, Poland) for providing the culture collection of human clinical isolates and to Ann Norton for technical assistance.

#### REFERENCES

- Alexander, E. H., and M. C. Hudson. 2001. Factors influencing the internalization of *Staphylococcus aureus* and impacts on the course of infections in humans. *Appl. Microbiol. Biotechnol.* **56**:361–366.
- Appelbaum, P. C. 2007. Microbiology of antibiotic resistance in *Staphylococcus aureus*. *Clin. Infect. Dis.* **45**:S165–S170.
- Archer, G. L. 1998. *Staphylococcus aureus*: a well-armed pathogen. *Clin. Infect. Dis.* **26**:1179–1181.
- Baba, T., T. Bae, O. Schneewind, F. Takeuchi, and K. Hiramatsu. 2008. Genome sequence of *Staphylococcus aureus* strain Newman and comparative analysis of staphylococcal genomes: polymorphism and evolution of two major pathogenicity islands. *J. Bacteriol.* **190**:300–310.
- Berthold, H., B. Frorath, M. Scanarini, C. C. Abney, B. Ernst, and W. Northemann. 1992. Plasmid pGEX-5T: an alternative system for expression and purification of recombinant proteins. *Biotechnol. Lett.* **14**:245–250.
- Bevers, L. E., M. W. H. Pinkse, P. D. E. M. Verhaert, and W. R. Hagen. 2009. Oleate hydratase catalyzes the hydration of a nonactivated carbon-carbon bond. *J. Bacteriol.* **191**:5010–5012.
- Chevallet, M., V. Santoni, A. Poinas, D. Rouquié, A. Fuchs, S. Kieffer, M. Rossignol, J. Lunardi, J. Garin, and T. Rabilloud. 1998. New zwitterionic detergents improve the analysis of membrane proteins by two-dimensional electrophoresis. *Electrophoresis* **19**:1901–1909.
- DeLeo, F. R., L. A. Allen, M. Apicella, and W. M. Nauseef. 1999. NADPH oxidase activation and assembly during phagocytosis. *J. Immunol.* **163**:6732–6740.
- Dziewanowska, K., A. R. Carson, J. M. Patti, C. F. Deobald, K. W. Bayles, and G. A. Bohach. 2000. Staphylococcal fibronectin binding protein interacts with heat shock protein 60 and integrins: role in internalization by epithelial cells. *Infect. Immun.* **68**:6321–6328.
- Fekkes, P., and A. J. Driessen. 1999. Protein targeting to the bacterial cytoplasmic membrane. *Microbiol. Mol. Biol. Rev.* **63**:161–173.
- Fischetti, V. A., R. P. Novick, J. J. Ferretti, D. A. Portnoy, and J. J. Rood. 2000. Gram-positive pathogens. ASM Press, Washington, DC.
- Foster, T. J. 2004. The *Staphylococcus aureus* “superbug.” *J. Clin. Invest.* **114**:1693–1696.
- Fox, P. M., R. J. Lampen, K. S. Stumpf, G. L. Archer, and M. W. Climo. 2006. Successful therapy of experimental endocarditis caused by vancomycin-resistant *Staphylococcus aureus* with a combination of vancomycin and beta-lactam antibiotics. *Antimicrob. Agents Chemother.* **50**:2951–2956.
- Guérout-Fleury, A. M., K. Shazand, N. Frandsen, and P. Stragier. 1995. Antibiotic-resistance cassettes for *Bacillus subtilis*. *Gene* **167**:335–336.
- Hallin, M., A. Deplano, O. Denis, R. De Mendonça, R. De Ryck, and M. J. Struelens. 2007. Validation of pulsed-field gel electrophoresis and spa typing for long-term, nationwide epidemiological surveillance studies of *Staphylococcus aureus* infections. *J. Clin. Microbiol.* **45**:127–133.
- Hermann, M., M. E. Jaconi, C. Dahlgren, F. A. Waldvogel, O. Stendahl, and D. P. Lew. 1990. Neutrophil bactericidal activity against *Staphylococcus aureus* adherent on biological surfaces. Surface-bound extracellular matrix proteins activate intracellular killing by oxygen-dependent and -independent mechanisms. *J. Clin. Invest.* **86**:942–951.
- Hiraga, S., C. Ichinose, H. Niki, and M. Yamazoe. 1998. Cell cycle-dependent duplication and bidirectional migration of SeqA-associated DNA-protein complexes in *E. coli*. *Mol. Cell* **1**:381–387.
- Hovde, C. J., S. P. Hackett, and G. A. Bohach. 1990. Nucleotide sequence of the staphylococcal enterotoxin C3 gene: sequence comparison of all three type C staphylococcal enterotoxins. *Mol. Gen. Genet.* **220**:329–333.
- Kil, K. S., M. W. Cunningham, and L. A. Barnett. 1994. Cloning and sequence analysis of a gene encoding a 67-kilodalton myosin-cross-reactive antigen of *Streptococcus pyogenes* reveals its similarity with class II major histocompatibility antigens. *Infect. Immun.* **62**:2440–2449.
- Klevens, R. M., M. A. Morrison, J. Nadle, S. Petit, K. Gershman, S. Ray, L. H. Harrison, R. Lynfield, G. Dumyati, J. M. Townes, A. S. Craig, E. R. Zell, E. Fosheim, L. K. McDougal, R. B. Carey, S. K. Fridkin, and Active Bacterial Core Surveillance MRSA Investigators. 2007. Invasive methicillin-resistant *Staphylococcus aureus* infections in the United States. *JAMA* **298**:1763–1771.
- Kobayashi, S. D., J. M. Voyich, C. Burlak, and F. R. DeLeo. 2005. Neutrophils in the innate immune response. *Arch. Immunol. Ther. Exp. (Warsz.)* **53**:505–517.
- Kobayashi, S. D., K. R. Braughton, A. R. Whitney, J. M. Voyich, T. G. Schwan, J. M. Musser, and F. R. DeLeo. 2003. Bacterial pathogens modulate an apoptosis differentiation program in human neutrophils. *Proc. Natl. Acad. Sci. U. S. A.* **100**:10948–10953.
- Koreen, L., S. V. Ramaswamy, E. A. Graviss, S. Naidich, J. M. Musser, and B. N. Kreiswirth. 2004. *spa* typing method for discriminating among *Staphylococcus aureus* isolates: implications for use of a single marker to detect genetic micro- and macrovariation. *J. Clin. Microbiol.* **42**:792–799.
- Kreiswirth, B. N., S. Löfdahl, M. J. Betley, M. O’Reilly, P. M. Schlievert, M. S. Bergdoll, and R. P. Novick. 1983. The toxic shock syndrome exotoxin structural gene is not detectably transmitted by a prophage. *Nature* **305**:709–712.
- Kuroda, M., T. Ohta, I. Uchiyama, T. Baba, H. Yuzawa, I. Kobayashi, L. Cui, A. Oguchi, K. Aoki, Y. Nagai, J. Lian, T. Ito, M. Kanamori, H. Matsumaru, A. Maruyama, H. Murakami, A. Hosoyama, Y. Mizutani-Ui, N. K. Takahashi, T. Sawano, R. Inoue, C. Kaito, K. Sekimizu, H. Hiramatsu, S. Kuhara, S. Goto, J. Yabuzaki, M. Kanehisa, A. Yamashita, K. Oshima, K. Furuya, C. Yoshino, T. Shiba, M. Hattori, N. Ogasawara, H. Hayashi, and K. Hiramatsu. 2001. Whole genome sequencing of methicillin-resistant *Staphylococcus aureus*. *Lancet* **357**:1225–1240.
- Laemmli, U. K. 1970. Cleavage of structural proteins during the assembly of the head of bacteriophage T4. *Nature* **227**:680–685.
- Liu, G. Y., A. Essex, J. T. Buchanan, V. Datta, H. M. Hoffman, J. F. Bastian, J. Fierer, and V. Nizet. 2005. *Staphylococcus aureus* golden pigment impairs neutrophil killing and promotes virulence through its antioxidant activity. *J. Exp. Med.* **202**:209–215.
- Lowy, F. D. 1998. *Staphylococcus aureus* infections. *N. Engl. J. Med.* **339**:520–532.
- Maalej, S., I. Dammak, and S. Dukan. 2006. The impairment of superoxide dismutase coordinates the derepression of the PerR regulon in the response of *Staphylococcus aureus* to HOCl stress. *Microbiol.* **152**:855–861.
- Malachowa, N., A. Sabat, M. Gniadkowski, J. Krzyszton-Russjan, J. Empel, J. Miedzobrodzki, K. Kosowska-Shick, P. C. Appelbaum, and W. Hryniewicz. 2005. Comparison of multiple-locus variable-number tandem-repeat analysis with pulsed-field gel electrophoresis, *spa* typing, and multilocus sequence typing for clonal characterization of *Staphylococcus aureus* isolates. *J. Clin. Microbiol.* **43**:3095–3100.
- McAleese, F., S. W. Wu, K. Sieradzki, P. Dunman, E. Murphy, S. Projan, and A. Tomasz. 2006. Overexpression of genes of the cell wall stimulin in clinical isolates of *Staphylococcus aureus* exhibiting vancomycin-intermediate-*S. aureus*-type resistance to vancomycin. *J. Bacteriol.* **188**:1120–1133.
- McCormick, J. K., T. J. Tripp, G. M. Dunny, and P. M. Schlievert. 2002. Formation of vegetations during infective endocarditis excludes binding of bacterial-specific host antibodies to *Enterococcus faecalis*. *J. Infect. Dis.* **185**:994–997.
- McDevitt, D., P. Francois, P. Vaudaux, and T. J. Foster. 1994. Molecular characterization of the clumping factor (fibrinogen receptor) of *Staphylococcus aureus*. *Mol. Microbiol.* **11**:237–248.
- Nauseef, W. M. 2007. How human neutrophils kill and degrade microbes: an integrated view. *Immunol. Rev.* **219**:88–102.
- Nickerson, N. N., L. Prasad, L. Jacob, L. T. Delbaere, and M. J. McGavin. 2007. Activation of the SspA serine protease zymogen of *Staphylococcus aureus* proceeds through unique variations of a trypsinogen-like mechanism and is dependent on both autocatalytic and metalloprotease-specific processing. *J. Biol. Chem.* **282**:34129–34138.
- Palazzolo-Ballance, A. M., M. L. Reniere, K. R. Braughton, D. E. Sturdevant, M. Otto, B. N. Kreiswirth, E. P. Skaar, and F. R. DeLeo. 2008. Neutrophil microbicides induce a pathogen survival response in community-

- associated methicillin-resistant *Staphylococcus aureus*. *J. Immunol.* **180**:500–509.
37. Rakita, R. M., N. N. Vanek, K. Jacques-Palaz, M. Mee, M. M. Mariscalco, G. M. Dunny, M. Snuggs, W. B. Van Winkle, and S. I. Simon. 1999. *Enterococcus faecalis* bearing aggregation substance is resistant to killing by human neutrophils despite phagocytosis and neutrophil activation. *Infect. Immun.* **67**:6067–6075.
  38. Rollof, J., and S. Normark. 1992. In vivo processing of *Staphylococcus aureus* lipase. *J. Bacteriol.* **174**:1844–1847.
  39. Rooijackers, S. H. M., K. P. M. van Kessel, and J. A. G. van Strijp. 2005. Staphylococcal innate immune evasion. *Trends Microbiol.* **13**:596–601.
  40. Ruppitsch, W., A. Indra, A. Stöger, B. Mayer, S. Stadlbauer, G. Wewalka, and F. Allerberger. 2006. Classifying spa types in complexes improves interpretation of typing results for methicillin-resistant *Staphylococcus aureus*. *J. Clin. Microbiol.* **44**:2442–2448.
  41. Sabat, A., J. Krzyszton-Russjan, W. Strzalka, R. Filipek, K. Kosowska, W. Hryniewicz, J. Travis, and J. Potempa. 2003. New method for typing *Staphylococcus aureus* strains: multiple-locus variable-number tandem repeat analysis of polymorphism and genetic relationships of clinical isolates. *J. Clin. Microbiol.* **41**:1801–1804.
  42. Sau, S., J. Sun, and C. Y. Lee. 1997. Molecular characterization and transcriptional analysis of type 8 capsule genes in *Staphylococcus aureus*. *J. Bacteriol.* **179**:1614–1621.
  43. Schlievert, P. M., P. J. Gahr, A. P. Assimacopoulos, M. M. Dinges, J. A. Stoehr, J. W. Harmala, H. Hirt, and G. M. Dunny. 1998. Aggregation and binding substances enhance pathogenicity in rabbit models of *Enterococcus faecalis* endocarditis. *Infect. Immun.* **66**:218–223.
  44. Sibbald, M. J. J. B., A. K. Ziebandt, S. Engelmann, M. Hecker, A. de Jong, H. J. M. Harmsen, G. C. Raangs, I. Stokroos, J. P. Arends, J. Y. F. Dubois, and J. M. van Dijl. 2006. Mapping the pathways to staphylococcal pathogenesis by comparative secretomics. *Microbiol. Mol. Biol. Rev.* **70**:755–788.
  45. Tamura, K., J. Dudley, M. Nei, and S. Kumar. 2007. MEGA4: Molecular Evolutionary Genetics Analysis (MEGA) software version 4.0. *Mol. Biol. Evol.* **24**:1596–1599.
  46. van Belkum, A. 2006. Staphylococcal colonization and infection: homeostasis versus disbalance of human (innate) immunity and bacterial virulence. *Curr. Opin. Infect. Dis.* **19**:339–344.
  47. Volkov, A., A. Liavonchanka, O. Kamneva, T. Fiedler, C. Goebel, B. Kreikemeyer, and I. Feussner. 2010. Myosin cross-reactive antigen of *Streptococcus pyogenes* M49 encodes a fatty acid double bond hydratase that plays a role in oleic acid detoxification and bacterial virulence. *J. Biol. Chem.* **285**:10353–10361.
  48. Voyich, J. M., K. R. Braughton, D. E. Sturdevant, A. R. Whitney, B. Said-Salim, S. F. Porcella, R. D. Long, D. W. Dorward, D. J. Gardner, B. N. Kreiswirth, J. M. Musser, and F. R. DeLeo. 2005. Insights into mechanisms used by *Staphylococcus aureus* to avoid destruction by human neutrophils. *J. Immunol.* **175**:3907–3919.
  49. Weems, J. J. 2001. The many faces of *Staphylococcus aureus* infection. Recognizing and managing its life-threatening manifestations. *Postgrad. Med.* **110**:24–26, 29–31, 35–36.
  50. Yang, S. J., K. C. Rice, R. J. Brown, T. G. Patton, L. E. Liou, Y. H. Park, and K. W. Bayles. 2005. A LysR-type regulator, CidR, is required for induction of the *Staphylococcus aureus* *cidABC* operon. *J. Bacteriol.* **187**:5893–5900.

---

Editor: J. N. Weiser